

Characterization and CFD Analysis of Traditional Vessels of Kerala



B Venkata Subbaiah, Santosh G Thampi, Nimma Rambabu, V Mustafa, M Abdul Akbar

Abstract: In this study, analysis of the hull forms of traditional vessels in Kerala, viz., Snake boat, Uru and Houseboat have been studied. Ideal draft from wave cut analysis, estimation of drag forces, pressure and velocity contours on the surface of the hulls has been studied using a proposed 3-D model. The CFD package SHIPFLOW 5.1® has been used for the hydrodynamic analysis of ship/vessel in this work. The wave-elevation vectors (Kelvin wave pattern) at different Froude numbers and the different draft has been evaluated along the length of the vessel.

The results show that that out of the total drag force experienced by a Snake boat at the ideal draft, 66.8% is attributed to the frictional drag and only 33.2% is wave-making resistance drag. These values change to 73.1% and 26.9% respectively for Uru and 23.7% and 76.3% for a Houseboat. With regards to the magnitude of resistance drag values, the total resistance experience by an Uru when compared to Snake boat and Houseboat are 30.16 and 1.17 times respectively. It has also been found that the presence of the skeg improves the hydrodynamic performance of the Houseboat considerably. The findings will be useful to design these boats considering its specific applications.

Keywords: Snake boat, Houseboat, Uru, SHIPFLOW, Kelvin wave pattern

Nomenclature

- B Breadth (m)
- C_B Block coefficient
- C_F Frictional resistant coefficient
- C_p Pressure resistant coefficient
- C_T Total resistant coefficient
- F_n Froude number
- L_{pp} Length between perpendiculars of the model (m)
- Re Reynolds number
- R_F Frictional resistance (N)
- R_n Reynolds number
- R_T Total resistant (N)
- S Wetted surface area (m²)
- T Draft (m)

Revised Manuscript Received on May 30, 2020.

* Correspondence Author

B Venkata Subbaiah*, Civil Engineering, National Institute of Technology Calicut, Calicut, India. Email: anandasainite@gmail.com

Santosh G Thampi, Civil Engineering, National Institute of Technology Calicut, Calicut, India. Email: santosh@nitc.ac.in

Nimma Rambabu, Civil Engineering, National Institute of Technology Calicut, Calicut, India. Email: nrb.369@gmail.com

V Mustafa, Civil Engineering, National Institute of Technology Calicut, Calicut, India. Email: mustafa@nitc.ac.in

M Abdul Akbar, Civil Engineering, Dr. B.R. Ambedkar National Institute of Technology, Jalandhar, India. Email: maakbar83@yahoo.co.in

© The Authors. Published by Blue Eyes Intelligence Engineering and Sciences Publication (BEIESP). This is an open access article under the CC BY-NC-ND license (<http://creativecommons.org/licenses/by-nc-nd/4.0/>)

- T Displacement (m)
- ρ Fluid density (kg/m³)
- η Fluid viscosity (m²/s)
- CFD Computational fluid dynamics
- PAF Panel method applied to free surface
- RANS Reynolds averaged Navier-stokes
- Re Reynolds number
- SA Spalart-Allmaras equation
- SST Shear stress transport
- VOF Volume of fluid

I. INTRODUCTION

The industrial revolution of the nineteenth century and the rapid expansion of water transportation, seafaring, and shipbuilding that followed brought the issue of safety to the limelight. In view of the growing number of vessels at sea, the risk involved in seafaring has been an overwhelming challenge. In India, Kerala State occupies a strategic location connecting the eastern and western worlds in the Indian Ocean region. Internal processes and external influences have facilitated the development of a vibrant maritime culture in the state, including interesting watercraft types, when compared to other regions in India. In traditional design methods, lots of model tests are required and thus it is costly and time-consuming. So, engineers turn to advanced numerical tools to aid their engineering design. However, in the ship industry, due to the existence of a free surface and the complex ship geometry, CFD has lagged behind other industrial fields. But with the recent breakthrough in ship CFD technology, practical applications of CFD in analyzing and predicting ship performance now become possible [1]. Many studies involving CFD applications to problems on the evaluation of resistance and stability of hull forms have been reported. Numerical simulation of the free-surface flow around a model naval ship, DTMB 5415, has been performed using FLUENT in [2].

Several significant problems have been encountered during the work and have been summarized to facilitate future applications of the code to similar naval problems. The resistance characteristics of six ships with different hull forms have been numerically studied using the solver FOAM-SJTU in [3].

Calculations for two typical benchmark surface ship models, Wigley and DTMB 5415, has been carried out for model validation. The numerical results have been compared with the experimental data and thereafter the model has been used to study the influence of Froude number on wave resistance and wave pattern. CFDSHIP-IOWA, a general-purpose unsteady Reynolds-averaged Navier-Stokes CFD code subsequently developed to handle a broad range of problems involving ship hydrodynamics has been introduced in [4].

The equations for viscous free surface considering nonlinear free surface boundary conditions have been formulated in [5]. These equations are used for predicting the damping of a freely sloshing viscous fluid for a range of Reynold number $3 \leq Re \leq 3 \times 10^5$. RANS simulation of free-surface flow around the modern ships DTMB 5415 U.S. Navy has been performed using the commercial CFD software namely FLUENT, using hybrid unstructured grids [6]. An investigation on the influence of finite depth on the wave-making characteristics of ships using a potential based panel method has been performed and reported in [7]. A computer program Panel-method Applied to Free Surface (PAFS) has been employed to simulate the effect of the finite depth of water on the Wigley hull. The computed wave profiles and wave-making resistance has been compared with that of Inuid S-201 hull in [7].

The difficulties encountered in predicting resistances of ships based on Dawson's method has been explained in [8]. The modified Dawson's method has been used to improve the prediction of the wave pattern and wave-making resistance. The proposed method has been applied to two ships of the Korean Institute of Ship and Ocean Engineering (KRISO), including a tanker and a container ship. The predicted wave patterns and wave-making resistance has been compared with the model test results and good agreement has been observed. The resistance, sinkage, and trim of a container ship using the computational fluid dynamics software SHIPFLOW have been determined in [9]. The computational fluid dynamics (CFD) simulation of steady ship motions at different drift angles, yaw rates, rudder angles, and their combinations for the KRISO Very Large Crude Carrier 2 (KVLCC2) tanker ship has been performed in [10]. The effect of various characteristics of the hull form of a ship on the added resistance in waves and derived a simple (level 1 type) formula by determining the best fit between available experimental data for different types of hull forms has been considered in [11]. The proposed formula has been simplified to such an extent that by using only the main ship particulars and fundamental wave characteristics, the added resistance of the ship can be computed. Extensive validation of the proposed simplified formula has been carried out for different types of ships and the results have been compared to that obtained by the existing methods [11]. A general method based on Green's theorem has been developed to tackle wave-making problems in the time domain [12]. A method to evaluate the total resistance of the ship in a seaway has been proposed in [13]. Besides water resistance, the added resistance due to waves has been computed using the panel method; wind resistance was obtained using CFD and this was verified by open wind test and using a statistical formula. the speed loss factor and Energy Efficiency Operational Indicator (EEOI) as objectives have been optimized using the NSGA-II algorithm [13].

The effect of marine coatings and biofouling on ship resistance has been analyzed by performing CFD simulations of a full-scale three-dimensional KRISO Container Ship (KCS) [14]. The increase in the effective power of the full-scale KCS hull has been predicted to be 18.1% for a deteriorated coating or light slime whereas, with heavy slime, this has been predicted to be 38% at a speed of 24knots [14].

A computational tool has been developed to evaluate the performance of various types of commercial ships in terms of resistance and propulsion characteristics [15]. Eight different commercial ships that have been built in the last decade were analyzed in this study. The progressive development of the Inclined Keel Hull (IKH) in terms of hydrostatic and resistance performance with the help of CFD and large-scale model tests has been presented in [16]. It has been observed that the success of the 'Inclined Keel' application in large commercial vessels requires a fine balance amongst the minimal increase in the bare hull resistance, a maximum gain in the propulsive efficiency and satisfaction of other essential naval architectural and operational criteria [16]. An extension of the Morino's panel method for the computation of the wave-making resistance of a ship in which the Kelvin classical linearized free surface condition is employed has been presented in [17]. The resulting numerical modeling has been compared in terms of the wave profile and wave resistance for the Wigley hull with experimental results [17]. A complete RANS simulation of the free-surface flow around a model ship has been performed in [18], the VOF method being used for free surface treatment and the SST $k-\omega$ turbulence model has been employed for viscous flow simulation. Free surface flow around the Wigley and DTMB 5415 models has been analyzed at a single Froude number. The influence of the Froude number on wave resistance and wave pattern generated by the Series 60 ship model was evaluated using a numerical model and the results were compared with experimental data [18]. RANS simulations of the free-surface flow around modern ship hulls with advanced turbulence models and interface capturing schemes were also performed, which demonstrated issues related to computational stability such as grid quality and resolution [1]. Computational results obtained from a RANS model for viscous free surface flow along a typical S60 ship hull at different Froude numbers have been presented along with wake flow for a complex surface ship with various appendages [20].

A three-dimensional Finite Volume Method based model has been employed to determine the drag coefficient [21]. The drag coefficient at different Froude numbers in the case of steady turbulent flows was evaluated. A hybrid method for computing the hydrodynamic resistance of models/ships has been developed in the Laboratory for Ship and Marine Hydrodynamics of the National Technical University of Athens (NTUA) [22]. This model is suitable when the flow is not influenced by abrupt changes in geometry, as in the case of full ships (e.g. tankers or bulk-carriers). Computational results using this model have been shown reasonable agreement with the results of model studies [22]. A simple method for estimating trans critical wave resistance from trim has been presented in [23]. An unsteady Reynolds-averaged Navier-Stokes equation-based model has been developed to analyze sinkage [24] and trim effects for a steadily advancing surface ship. The volume of fluid (VOF) method was used for the treatment of the free surface. Sinkage and trim were predicted by using dynamic mesh technology; the motion of the ship is controlled by six degrees of freedom (6DOF).

Results pertaining to sinkage, trim and resistance at seven Froude numbers were compared with experimental data. Factors that affect ship resistances were identified and formulae for calculating ship resistance under different drafts, longitudinal trims and arbitrary drift-trim coupled running attitudes were defined [24]. The application of CFD methods for hull form optimization in a model basin has been reported [25]. The use of CFD methods for hull form optimization in a model basin, hull form modeling, and modification, and potential flow RANS computations have been reported [26]. Developments in CFD also enables wide acceptance of simulation to design the vessel shapes having low drag [27]. Applications of the immersed boundary (IB) method to simulate incompressible turbulent flows around complex configurations have been reported in [28]. The main features of the IB technique have been described with an emphasis on the treatment of boundary conditions at an immersed surface [28].

The possibility of mitigating surf-riding of the ITTC A2 fishing vessel in the design stage has been investigated in [29] using the 6-DoF weakly non-linear model developed for surf-riding simulations in quartering seas. The longitudinal position of the center of buoyancy (LCB) of the ship was chosen as the design parameter. Results show that surf-riding cannot be prevented by the adjusting LCB. To reduce fuel consumption and operating costs, a fishing boat optimization approach using a Computational Fluid Dynamics (CFD) technique [30] has been presented. Optimization results have been shown that the optimization loop presented in this study can be used to design a fishing boat that has a minimum total resistance in calm water [30]. Overall stability performance of alternative hull forms has been studied in [31, 32]. The effect of the variable buoyancy has been examined in terms of the gliding angle, velocity, and angle of attack [33].

Numerical simulation of ship stability for a dynamic environment has been performed in [34]. A nonlinear approach has been utilized to predict the roll response of an RO-RO ship. Various representations of damping and restoring terms found in the literature have been investigated here. A parametric investigation was undertaken to identify the effect of key parameters like wave amplitude, wave frequency, meta-centric height, etc. [34]. The wave resistance components for high-speed catamarans have been investigated in [35]. Two methods were applied: the slender-body theory and a 3D method. Results were obtained for different types of twin hulls and attention was given to the effects of catamaran hull spacing. The study also included the effects of shallow water on the wave resistance component.

From the literature review, it has been observed that very few efforts have been reported on documentation of traditional knowledge related to sailing vessels including the technology of shipbuilding. The studies on the hydrodynamic analysis of traditional hull forms of Kerala have not been reported. The basic requirements of vessels are high stability and low resistance. These requirements can be achieved by subjecting the hull forms to CFD analysis and modifying them based on the results of simulations until the designed performance standards are met. In the Indian scenario, there is

ample scope to improve the certification mechanism for vessels, in general, and certain categories of vessels in particular. The study proposed in this work could help in suggesting improvements to the criteria for the certification of vessels, thereby ensuring higher levels of safety. Considerable research has been reported on the analysis of hull forms; however, analysis of the hull forms of traditional vessels in Kerala has not yet been performed. In this study, the three prominent traditional vessels of Kerala, viz., Snake boat, Uru and Houseboat have been studied. Ideal draft from wave cut analysis, estimation of drag forces, pressure and velocity contours on the surface of the hulls has been studied using a proposed 3-D model.

II. HISTORICAL BACKGROUND AND SELECTION OF BOATS FOR THIS CURRENT STUDY

Kerala's strategic location connects the eastern and western worlds in the Indian Ocean region. Its internal processes and external influences have caused the development of vibrant maritime culture, including interesting watercraft types, with the Western Ghats on the east and the Arabian Sea on the west, Kerala is enriched by the monsoons, 44 perennial rivers, 15 backwaters, and a 600km coast. The average temperature is between 20° and 32° C, and the annual rainfall varies from 1800 to 3600mm. Kerala has rich sources of timber suitable for boat-building. Boat-building in Kerala, perhaps, extends to the prehistoric period. Movement and fishing in coastal regions have been essential for their subsistence.

Uru is an extremely large and well-built vessel (Fig. 1) made by connecting planks of teak wood manually [36]. During earlier times, teak wood used for building the Uru has been brought from the Nilambur forests. These vessels were in huge demand in the Middle East. At present, these wooden ships are built near very few minor ports in Kerala, one such port being Beypore in the river mouth of the Chaliyar, around 12km south of Kozhikode city. These boats were used by the Arabs, since ancient times as trading vessels. Even now, Uru is being manufactured and exported to Arab nations from Beypore. Not much attention has however been paid either to the history of these enterprises or to the details of this shipbuilding technology [37]. Consequently, the indigenous knowledge base of this boat and shipbuilding is fast slipping into oblivion. The naval tradition of India is a rich heritage worth conservation, renovation, and enrichment. Not only has the performance of these vessels has been scientifically studied, but also scope for improvements in the design has been explored much [38].



Fig. 1. Bow and stern views of Uru [36]

Snake boat is a marvelous example of ancient Indians prowess in Naval Architecture (Figs. 2a and 2b). these boats have become one of the important icons of Kerala culture in recent years. Vallamkali is a renowned racing spectacle that is held every year in Kerala in which snake boats are employed. Trained oarsmen in traditional attire compete in this race. The margins of victory are very narrow, the history of this race and the speed records are well documented. Traditionally, each boat belongs to a village, and the villagers worship that boat like a deity. Only men are allowed to touch and board the boat, and to show the respect they should be barefooted. To make the boat more slippery while in the water and thereby to reduce the resistance of the hull, it is oiled with a mixture of fish oil, coconut shell carbon, and eggs. Repair work is done annually by the village carpenter.



Fig. 2a. Snake boat in docked position. Fig. 2b. Snake boat used in racing (scenes from Vallamkali).

Fig. 3 shows a typical houseboat (Kettuvallom) which is widely used by the tourism industry in Kerala. It is a large floating vessel with high load carrying capacity and has been part of Kerala's culture and heritage over the years. Houseboats could sail harnessing wind energy. For centuries, the houseboat was an important mode of transportation in coastal Kerala facilitating accessibility to even the most remote areas. Due to its sheer size and shape, houseboats can carry the load, which is more than thrice that of a cargo truck. Kettuvalloms of Kerala are giant country crafts measuring up to 80 – 90ft in length. Kettuvalloms means a boat made by tying together pieces of wood. The entire boat is held together by knots, in which nails are not used. Jackwood or Anjili planks are joined together with coir rope and then coated with black resin made from boiled cashew nutshells.



Fig. 3. Houseboat [39]

The task of modeling these vessels was challenging as formal drawings of these has not been maintained and not available. Also, no literature pertaining to the hydrodynamics of these vessels could be traced during the literature review. The work involved field survey to collect data required for constructing 3-D models of these vessels, constructing the 3-D models using several commercially available software, converting these 3-D models to a format that could be input to the CFD package for performing the hydrodynamic analysis. The CFD package SHIPFLOW has been used here.

III. RESULTS AND DISCUSSION

A. Validation of the package used for the analysis

The CFD package SHIPFLOW 5.1® has been used for the hydrodynamic analysis of ship/vessel in this work. This software has been used by many ship designers for application ranging from optimization of ship fore bodies (bulb) for wave resistance to the design of energy-saving devices in self-propelled full-scale condition. It has the panel generator for the potential flow using the XMesh module. It solves the RANS equation using finite volume code through XCHAP.

It is important to validate the package before interpreting the results for the current research problem. Therefore, simulations were performed using data pertaining to the dimensions of standard U.S Navy vessel -Series 60 (S_60) hull [40] for validation of SHIPFLOW 5.1® which has been listed in Table 1. Fig. 4. presents the fine mesh around the S_60 hull generated in SHIPFLOW 5.1®. In this validation study, the size of the fluid domain employed is one L_{PP} from F.P., $1.5 L_{PP}$ from A.P. and a radius of $3 L_{PP}$. For a fair comparison, boundary conditions taken for the FLUENT package listed in Table 2 have been considered and simulated in SHIPFLOW 5.1®. Steady viscous flow around a ship hull with the free surface has been studied by solving the Reynolds-averaged Navier-Stokes (RANS) model equations numerically [28]. The mathematical model which is available in SHIPFLOW 5.1® has been taken and the boundary conditions listed in Table 2 have been used in developing the offset file of S_60 hull which has been depicted in Fig. 5.

The wave-elevation vectors (Kelvin wave pattern) at Froude numbers of 0.16, 0.20, 0.24, 0.28, 0.30 and 0.316 were evaluated along the length of the vessel. For a better understanding of Kelvin wave pattern variation with respect to Froude number, simulated results for Froude numbers 0.16, 0.24 and 0.316 are presented in Fig. 6 (a), (b) and (c) respectively. It has been observed that the width of the wave pattern at the bow and stern increases with an increase in speed.

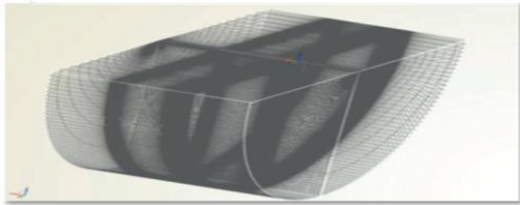


Fig. 4. Computational fluid domain.

Table 1. Prototype dimensions of S_60 Hull

Parameter	Length Between Perpendiculars (L_{PP})	Breadth (B)	Draft (T)	Block Coefficient (C_B)	Wetted surface area (S)
S_60 dimensions	121.92 m	16.26 m	6.502 m	0.60	2526.4 m ²

Table 2. Boundary conditions

	No-slip	Slip	Inflow	Outflow
u	$u_i = 0$	$u_i n_i = 0, \frac{\partial u_i}{\partial \xi_B} = 0$	$u_i = \text{constant}$	$\frac{\partial u_i}{\partial \xi_B} = 0$
p	$\frac{\partial p}{\partial \xi_B} = 0$	$\frac{\partial p}{\partial \xi_B} = 0$	$\frac{\partial p}{\partial \xi_B} = 0$	$p = 0$
k	$k = 0$	$\frac{\partial k}{\partial \xi_B} = 0$	$k = \text{constant}$	$\frac{\partial k}{\partial \xi_B} = 0$
ω	$\omega = f(u_\tau, \frac{\partial \omega}{\partial \xi_B} = 0$	$\frac{\partial \omega}{\partial \xi_B} = 0$	$\omega = \text{constant}$	$\frac{\partial \omega}{\partial \xi_B} = 0$



Fig. 5. Offset file of hull series 60 (S_60)

Fig. 7 (a), (b) and (c) show the wave profiles along the length of the ship/vessel for Froude numbers 0.16, 0.24 and 0.316 respectively. In these figures, the distance specified on the X and Y-axis is the normalized length (Wave profiles obtained using the XPAN module in SHIPFLOW 5.1® for potential flow is named as XPAN Wave profile in various Figures). At the Froude number of 0.316, the maximum wave height is $(0.022 \times L_{PP})$ 2.68 m; which is higher than the maximum wave height at lower Froude numbers of 0.24 and 0.16. As expected, the wave heights subside once the waves pass through the length of the boat. The computed wave profile generated through the motion of the boat at various Froude numbers is useful in the study of wave resistance.

The variation in the coefficient of wave-making resistance with Froude number obtained using published results [40] and compared with SHIPFLOW 5.1® package is depicted in Fig. 8. From the figure, the wave resistance is proportional to the Froude number; the higher the value of F_n , the higher the resistance. It has been observed that the wave-making resistance coefficient values computed using published results and SHIPFLOW 5.1® are in close agreement with

each other and hence the models developed in SHIPFLOW 5.1® have been validated.

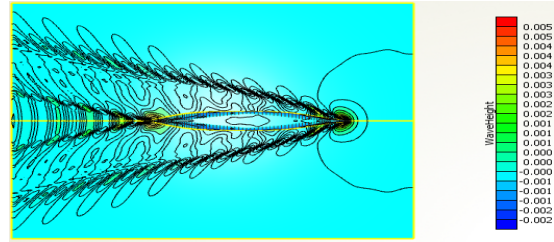


Fig. 6(a). Kelvin wave pattern at $F_n = 0.16$

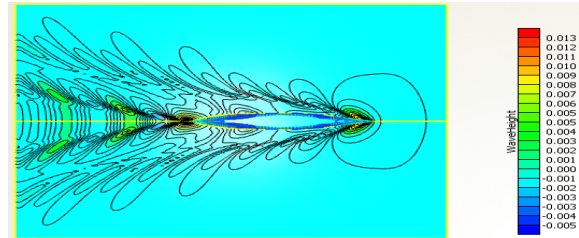


Fig. 6(b). Kelvin wave pattern at $F_n = 0.24$

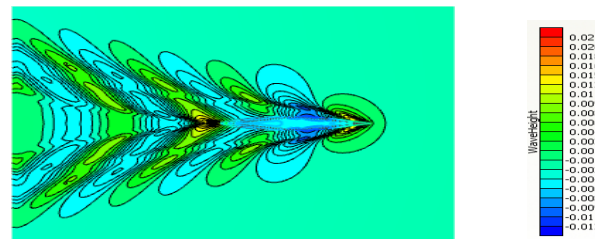


Fig. 6(c). Kelvin wave pattern at $F_n = 0.316$

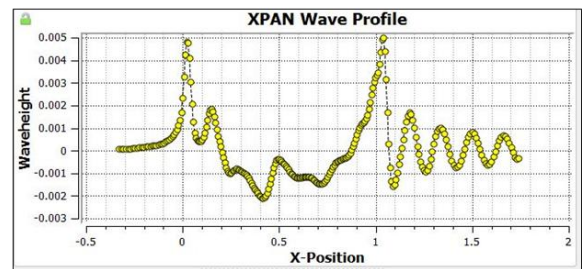


Fig. 7(a). Wave profile at $F_n = 0.16$

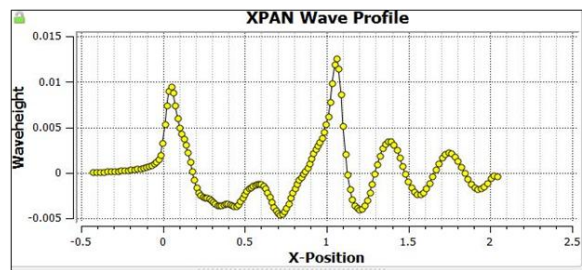


Fig. 7(b). Wave profile at $F_n = 0.24$

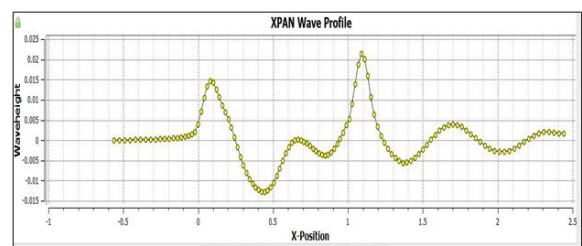


Fig. 7(c). Wave profile at $F_n = 0.316$

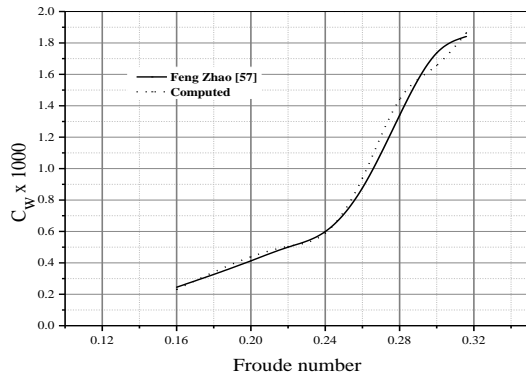


Fig. 8. Comparison of C_w values

B. Characterization and CFD Analysis of a Typical Snake Boat

The model of the boat has been analyzed in SHIPFLOW 5.1®. For finding the wave-making drag, the computational domain has been divided into two grids; one on the ship hull surface and other on the water surface using the XPAN module in SHIPFLOW 5.1®. Flow lines, wave profile along the length of ship and wave-making resistance have been computed. The analysis has been performed for coarse, medium and fine meshes and different combinations of draft and Froude numbers. For the computation of viscous drag, the domain has been subdivided into a finite number of cells. The analysis has been carried out using the XCHAP module in SHIPFLOW 5.1®. The flow has been computed with a double model ($k - \epsilon$ and $k - \omega$) with a prescribed free-surface for coarse, medium and fine meshes. The prototype dimensions and hydrostatic particulars of the snake boat have been shown in Table 3 and Table 4 respectively.

Table 3. Prototype dimensions of Snake Boat

Parameter	Length between perpendiculars L_{pp} (m)	Breadth B (m)	Draft T (m)	Block Coefficient C_B	Surface area S (m^2)
Vaues	19.695	2.32	0.787	0.38	30.528

Table 4. Hydrostatic particulars of snake boat

Draft Amidships m	0.1	0.2	0.3	0.4	0.5	0.6	0.7
Displacement, t	0.38	1.42	3.02	5.07	7.54	10.3	13.51
Draft at FP, m	0.10	0.20	0.30	0.40	0.50	0.60	0.70
WL Length, m	9.40	13.6	16.0	18.0	19.8	21.3	22.8
Beam max extents on WL, m	0.97	1.37	1.61	1.78	1.94	2.08	2.24
Wetted Area, m^2	7.08	13.7	19.5	24.9	30.2	35.7	41.4
Waterpl. Area, m^2	6.87	12.9	17.8	21.8	25.5	29.0	32.4

Fig. 9 depicts the iteration history plot for the analysis

carried out. The results of the XCHAP analysis are presented in Table 5.

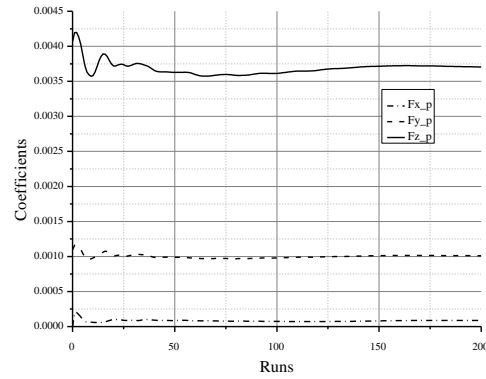


Fig. 9. XCHAP run history plot

Table 5. XCHAP results

Resistance Coefficients		CONDITIONS	
C_F (Frictional resist. coeff.)	0.002095	$V_{m,s}$ (Speed [m/s])	4.035
C_p (Pressure resist. coeff.)	0.000385	L_{ref} (Reference length [m])	19.69
C_T (Total resist. coeff.)	0.002145	F_n (Froude number)	0.29
S (Wetted surface [m^2])	30.295	R_n (Reynolds number)	9,42,40,000
HULL DATA		ρ (Fluid density [kg/m^3])	1026
L_{pp} (Model [m])	19.69	η (Fluid viscosity [m^2/s])	1.189×10^{-6}
S (Wetted area [m^2])	30.295	g (Gravity [m/s^2])	9.807
RESISTANCE			
R_F (Frictional resistance [kN])	530.101	R_T (Total resistance [kN])	542.75

The model was run initially with coarse and medium-sized meshes to ascertain errors in the model as the run times were slower. After rectification of errors, the model was finally run with a fine mesh to obtain accurate results. Fig. 10 and Fig. 11 depict a comparison of the coefficient of wave-making resistance for different mesh sizes for drafts of 0.5m and 0.6m respectively.

From Fig. 10, the average percentage deviation of C_w values between coarse and medium mesh was 10.15% and that medium and fine mesh was 2.4% for a draft of 0.5m. Similarly for a draft of 0.6m, the computed average percentage deviation of C_w values shown in Fig. 11 between coarse and medium mesh was 8.16% and that medium and fine mesh was 2.13%. The reduction in the percentage deviation in the medium and fine mesh when compared with the coarse and medium mesh is a clear indication of the convergence of the values. Though the computational time taken to simulate the fine mesh is more, the simulation results obtained are more accurate as compared with the other two meshes.

Fig. 12 presents the computational domain discretized with fine mesh around the snake boat with 1050504 cells and 939330 nodal points, the size of the fluid domain being L_{pp} from F.P., $1.5 L_{pp}$ from A.P. and having a radius of $4 L_{pp}$. Though $3 L_{pp}$ is generally acceptable as per ITTC recommendation, $4 L_{pp}$ was employed in the present analysis subsidiary high speeds and deeper flow disturbance. Fig. 13 presents a 3-D view of the Kelvin wave pattern at $C_w = 0.24$ and for a draft of 0.5m.

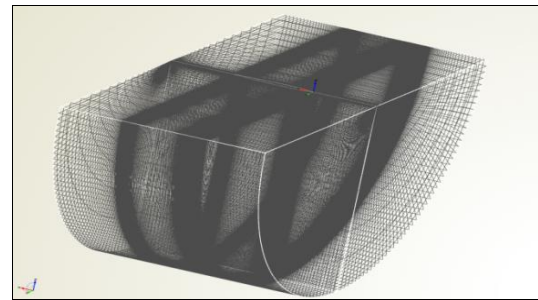


Fig. 12. Meshing of fluid domain around snake boat

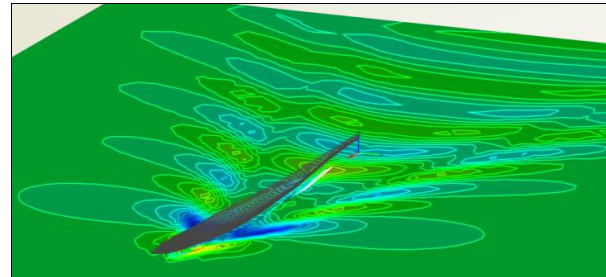


Fig. 13. A 3-D view of the Kelvin wave pattern

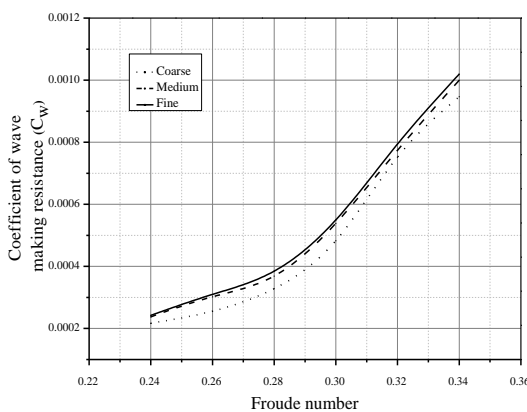


Fig. 10. Comparison of C_w values for different mesh sizes (draft = 0.5m)

Analyses were performed for drafts of 0.5m and 0.6m and Froude number ranging from 0.24 to 0.34 (at an increment of 0.20). The analysis has been performed for the boundary conditions presented in Table 2.

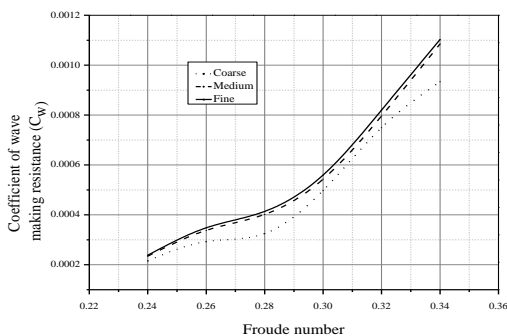


Fig. 11. Comparison of C_w values for different mesh sizes (draft = 0.6m)

Fig. 14 presents the Kelvin wave pattern (wave contours) and wave profiles at Froude numbers 0.24, 0.280, and 0.30. The variation in the wave pattern as the wave propagates away from the hull can be observed, and the wave cuts along the length of the boat increase with speed. The wave height increases significantly from bow to stern, the longitudinal profile of the snake boat also rises from the mid-point to the stern, and hence there is no risk involved even for the raised wave. From Fig. 14, it is clear that the wave profile near the bow starts with a trough for lower Froude numbers and changes to crest with the increase in Froude number. From the figure, the wave pattern contains both transverse and diverging waves at all speeds of the ship.

Fig. 15 is a plot of the position of the top of the boat with respect to sea level versus Froude number for 0.5m and 0.6m drafts. As evident from Fig. 15(b), for a draft of 0.6m, the wave surface elevation is crossing the top of the vessel beyond a certain Froude number. It indicates that the boat is under trouble due to sinking by the effect of the wave which is unacceptable. Hence, the design draft for the boat needs to be limited to 0.5m and this condition shall have strictly adhered for Froude numbers from 0.24 to 0.34; wherein, the higher value corresponds to the maximum value of velocity attained 17.03kmph, which marginally falls short of velocity attained by the record holder (19.76kmph) in the long history of snake boat race [41].

Figs. 16(a) to (f) and Figs. 17(a) to (f) are plots of pressure and velocity coefficients respectively along the length of the boat. The non-dimensionalized pressure is extracted through the expression, $p = 0.5C_p p_0$ (measured in Pascals, $p_0 =$ atmospheric pressure 101325Pa) and the non-dimensionalized velocity is extracted by multiplying with the ship speed. These offer, useful information regarding pressure and velocity and are useful for improving the ship lines.

A C_p value of zero indicates that the pressure is the same as the free stream pressure, a C_p value of one indicates the pressure is stagnation pressure and the point is a stagnation point and a C_p value of minus one (-1) indicates a perfect location for "Total energy".

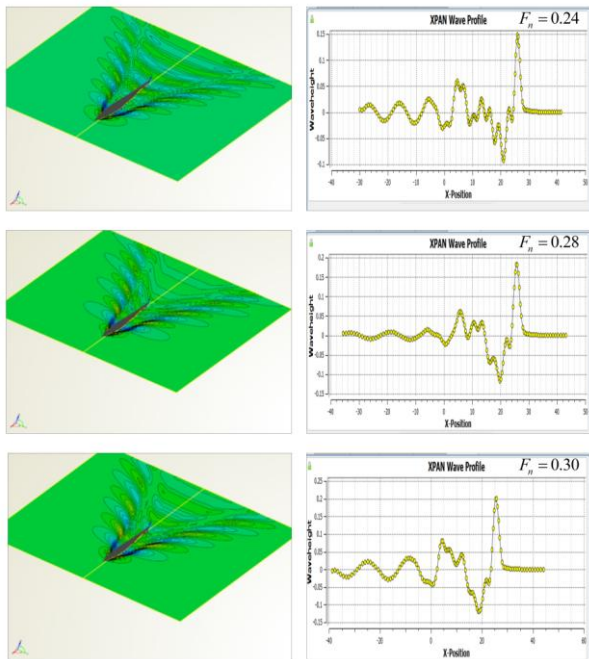


Fig. 14. Kelvin wave pattern and wave profile for 0.5m draft

By observing the pressure contours (Fig. 16 (a)) for $F_n = 0.24$, it can be observed that at the bow and the stern, the vessel experiences a pressure of 5420.89Pa (green colored values corresponding to a scale value of 0.107), most parts of the hull surface experience a pressure of about 506.63Pa (aqua-colored values corresponding to the scale value of 0.010); the first half portion of the vessel experiences a negative pressure of 303.98Pa (blue colored values corresponding to a scale of -0.006) and also a suction pressure of 7092.75Pa. When pressure increases, velocity will decrease and drag force will increase, thereby affecting fuel efficiency. By observing velocity profiles in Fig. 17(a) to (f), it is observed that the turbulence of water on the hull surface increases with an increase in Froude number. Turbulence is an indicative parameter of wave resistance; the higher the turbulence, the higher the wave resistance.

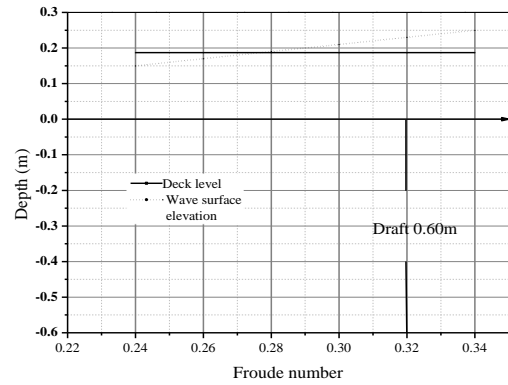
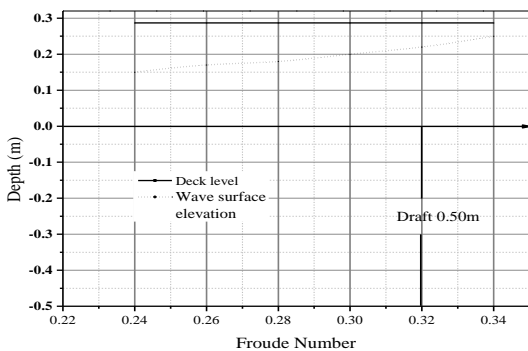


Fig. 15. Froude number versus freeboard at (a) draft = 0.5m and (b) draft = 0.6m

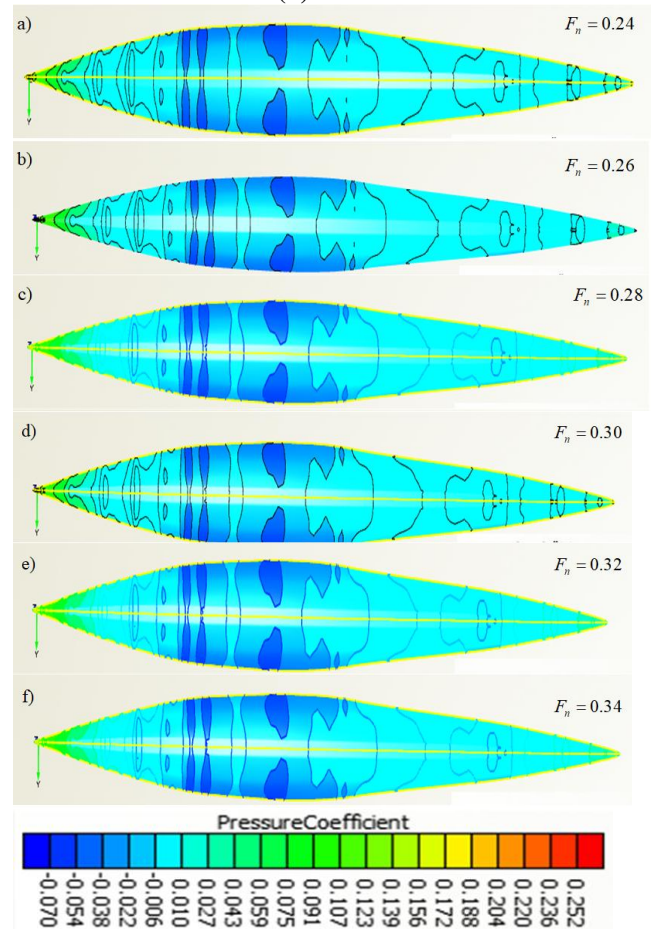
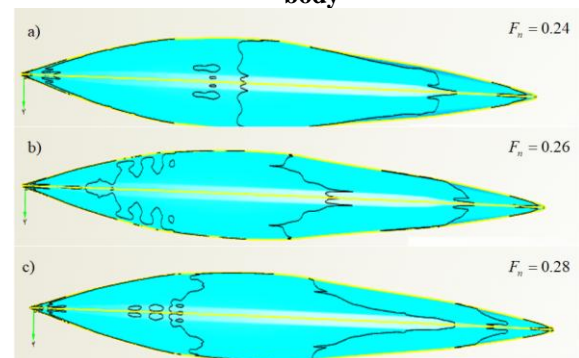


Fig. 16. Pressure coefficient contours on the surface of the body



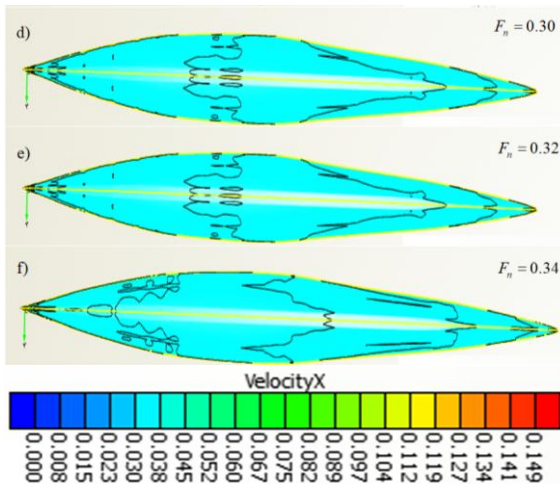


Fig. 17. Velocity coefficient contours on the surface of the body

The computed values of resistance coefficients for the snake boat analyzed are tabulated in Table 6. These values are used to the comparison of different vessels for their performance. It is useful in computing the resistance encountered by the vessels and comparing the resistance encountered by different vessels. Fig. 18 presents the wave-making drag, frictional drag and total drag on the snake boat considered in this study at a design draft 0.5m at different Froude numbers. It has been observed that the maximum values of wave-making drag, frictional drag, and total drag are 178.2kN, 358.3kN and 536.6kN respectively, at Froude number of 0.34. From the figure, it has been observed that although the general trend of resistance is to increase with increasing Froude number, there has been a reversal of this trend for the Froude number of 0.28. This has been explained by the variation in the wetted surface area with a change in vessel speed.

Table 6. Computed values of resistance coefficients for a typical snake boat

F_n	0.24	0.26	0.28	0.30	0.32	0.34
C_w	0.00215	0.0021	0.0021	0.0020	0.0020	0.0020
C_F	0.00230	0.0022	0.0021	0.0021	0.0020	0.0020
C_T	0.00444	0.0043	0.0042	0.0042	0.0041	0.0041

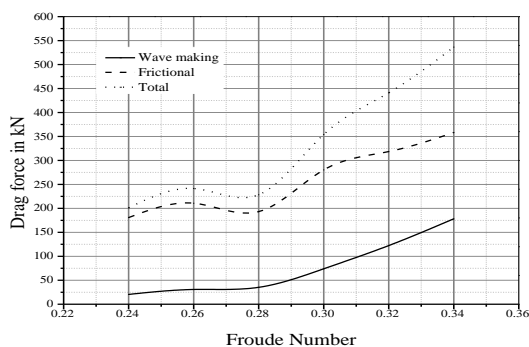


Fig. 18. Drag force versus Froude number

C. Characterisation and CFD Analysis of a Typical Uru Boat

In the computation of viscous drag, the domain has been subdivided into a finite number of cells. The analysis has been carried out using the XCHAP module in SHIPFLOW 5.1®. XCHAP module has been chosen over XPAN models as the computations involved the calculation of viscous components as well. The prototype dimensions and draft amidship parameters have been presented in Table 7 and 8 respectively. The results of XCHAP results are given in Table 9. The XCHAP iteration history plot for 2.4m draft and Froude number of 0.225 is shown in Fig. 19.

Table 7. Prototype dimensions of Uru

Parameter	Length between perpendiculars L_{PP} (m)	Breadth (B) (m)	Draft (T) (m)	Block Coefficient (C_B)	Surface area (S) (m^2)
Values	31.12	10.14	3.92	0.467	315.12

Table 8. Hydrostatic particulars of Uru

Draft	1.131	1.22	1.319	1.413	1.50	1.6	1.6
Amidships m	5	5	5	5	6	6	6
Displacement, t	39.05	52.0	66.75	82.87	100.	118	137
Draft at FP, m	1.13	1.22	1.319	1.413	1.50	1.6	1.6
Draft at AP, m	1.13	1.22	1.319	1.413	1.50	1.6	1.6
Draft at LCF, m	1.13	1.22	1.319	1.413	1.50	1.6	1.6
WL Length, m	30.49	30.6	30.81	30.97	31.1	31.	31.
Beam max extents on WL, m	8.09	8.52	8.833	9.079	9.28	9.4	9.5
Wetted Area, m^2	172.3	193	211.5	227.2	238.	250	261

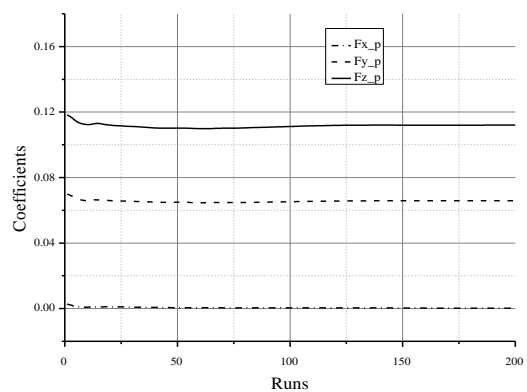


Fig. 19. XCHAP run history plot

Table 9. XCHAP results

Resistance Coefficients		Table 9. XCHAP results	
		CONDITIONS	
C_F (Frictional resist. coeff.)	0.002071	$V_{m,s}$ (Speed [m/s])	3.601
C_P (Pressure resist. coeff.)	0.002774	L_{ref} (Reference length [m])	31.12
C_T (Total resist. coeff.)	0.004845	F_n (Froude number)	0.2061
S (Wetted surface [m ²])	0.3484	R_n (Reynolds number)	9,42,40,000
HULL DATA		ρ (Fluid density [kg/m ³])	1026
L_{pp} (Model Lpp [m])	31.12	η (Fluid viscosity [m ² /s])	1.189*10 ⁻⁶
S (Wetted area [m ²])	337.4	g (Gravity [m/s ²])	9.807
RESISTANCE			
R_F (Frictional resistance [kN])	4.649	R_T (Total resistance [kN])	10.87

The model was initially run with coarse and medium meshes to get an overall idea of the behavior and to enable rectification of errors; also, the run times were lower when compared to the run employing fine meshing. After rectification of errors, the model was finally run with a fine mesh to obtain accurate results. The run time for the Uru has been larger when compared to that of the snake boat, owing to the larger problem size (11,867,744 cells as against 1,050,504 cells for snake boat) necessitating more refined meshing to capture the flow physics as accurately as possible.

The variation in the wave pattern as the wave propagates away from the hull can be observed from Fig. 20. The width of propagation increases significantly towards the stern and the wave cuts along the length of the Uru increases with speed. It has been observed that the wave pattern consists of transverse and diverging waves. It is evident that the wave height is increasing with the increase in the Froude number.

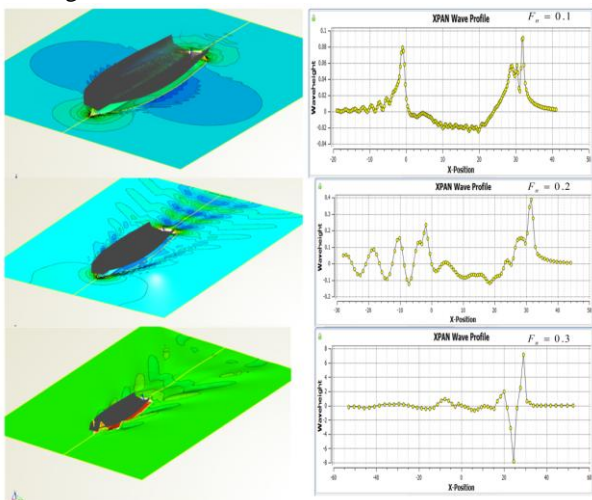


Fig. 20. Kelvin wave pattern and wave profile at different Froude numbers

Plots of top of the vessel with respect to sea level versus Froude number for 2.4m and 2.5m drafts are presented in Fig. 21 and 22 respectively. It is evident from Fig. 22 for a draft of 2.5m the wave surface elevation is crossing the top of the vessel beyond a certain Froude number. It indicates that the boat is under trouble due to sinking by the effect of the wave which is unacceptable. Hence, the design draft for the boat needs to be limited to 2.4m and this condition shall have strictly adhered to Froude numbers from 0.10 to 0.35 (speeds between 6.29kmph to 22.00kmph). Designers can use this ideal draft to determine the weight that the vessel can carry.

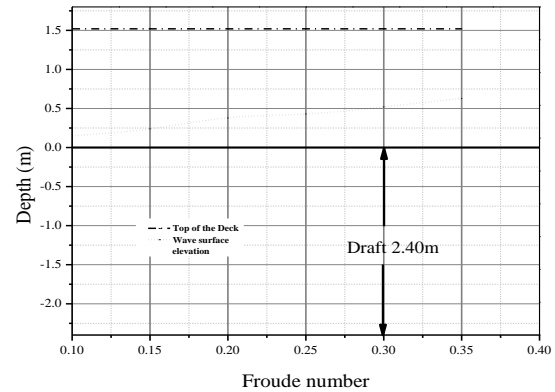


Fig. 21. Plot of wave surface elevation versus the top of the vessel for a draft of 2.4m

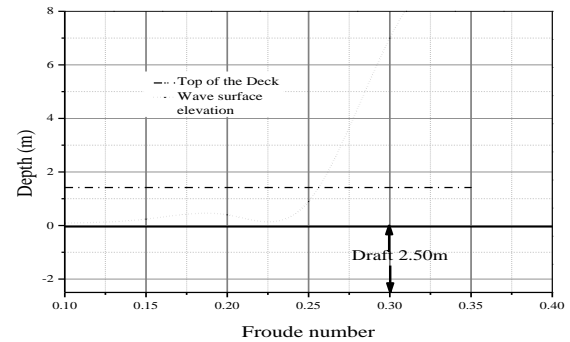


Fig. 22. Plot of wave surface elevation versus the top of the vessel for a draft of 2.5m

The curved surface of the vessel known as the skeg has arrived at the best of our knowledge through traditional wisdom without any formal analysis. To assess the performance of the Uru with a traditional skeg with that of one with a linear surface, two sets of analyses have been carried out. The first set of analyses has been performed maintaining the traditional shape of the skeg (which will be referred to as “with skeg” case); in the second case, the curved shape has been replaced by a linear surface (referred to as “without skeg” case).

Pressure and velocity contours have been obtained corresponding to Froude numbers of 0.15, 0.18, 0.21 and 0.24 for a design draft of 2.4m. Figs. 23 to 26 are plots of pressure and velocity contours along the length of the vessel for ‘with skeg’ and ‘without skeg’ cases for Froude numbers of 0.15 and 0.24. The pressure and velocity are computed as given in the previous snake boat, which is useful for optimizing the shape of Uru.

By observing the pressure contours in Fig. 23(a), it can be seen that there is a uniform suction pressure of around 4250Pa covering most parts of the hull and a pressure value of around 24200Pa at the edge of the bow and stern. These maximum values of pressure are a good input for designers to decide the material of the vessel. Although the pressure is much lesser than the design strength of the material, the fatigue aspect of the pressure should be considered and hence a stronger material should be used to build the vessel at locations where the pressure is more and economically lower strength materials can be used at locations where the pressures are lesser.

From Fig. 24(a), it has been observed that the pressure values are not as uniform as in Fig. 23(a). Moreover, the area experiencing maximum positive pressure (covering the bow and stern portion) has increased. Therefore, it can be inferred that the pressure on the surface of the vessel is higher in the case without a skeg, resulting in a reduction in velocity and an increase in drag force.

From the velocity profiles presented in Fig. 25(a), it is noted that there is a uniform flow velocity of almost 0.10m/sec covering most parts of the hull surface with small pockets of turbulence. In the case of “without skeg” (Fig. 26(a)), it is observed that the velocity on the surface is not as uniform when compared to that in Fig. 25(a). Therefore, based on both the pressure and velocity contours obtained, it can be concluded that the presence of the skeg improves the hydrodynamic performance of the vessel considerably. The increased uniformity of velocity contours for the skeg case is a clear indication of a better-streamlined shape for the vessel. The absence of skeg would mean greater turbulence for the Uru.

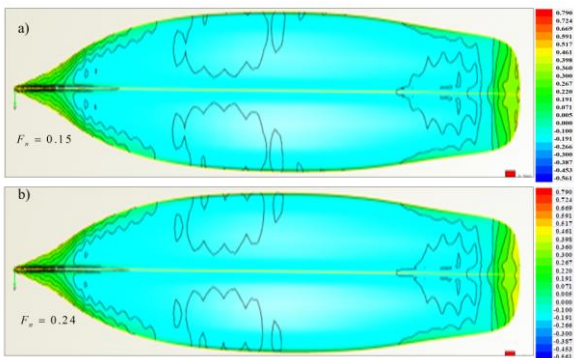


Fig. 24. Pressure contours on the surface without skeg



Fig. 25. Velocity contours at the bottom of the vessel with skeg

To formalize the results for the Uru, the analysis has been carried out for Froude numbers from 0.1 to 0.35. The analysis has also been carried out for the Froude number of 0.23 which is the average value for the range considered (0.1 to 0.35). Figs. 27(a) and 27(b) present the pressure and velocity contours respectively for the Froude number of 0.23 (which corresponds to a speed of 7.81knots or 14.46kmph). The draft used in this analysis was the ideal design draft of 2.4m obtained from Fig. 22. It has been observed that the pressure attains a maximum value of 19454Pa at edges of the forebody however it remains constant in the after body with a magnitude of around 800Pa. The velocity contours indicate different (but uniform) velocities over the two halves of the Uru, suggesting that the Uru is in a balanced position on the water surface without overly tilting (corresponding to pitch) to either of the ends.

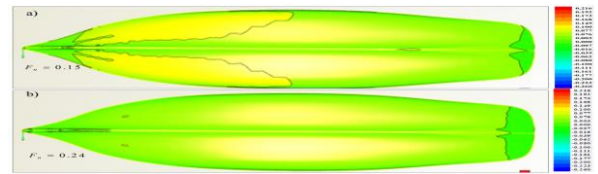


Fig. 26. Velocity contours at the bottom of the vessel without a skeg

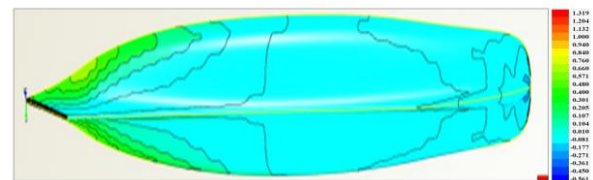


Fig. 27(a). Pressure at design speed with skeg

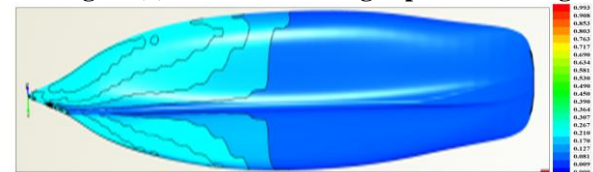


Fig. 27(b). Velocity at design speed with skeg

The streamline pattern and pressure at the bow and stern portions for the design draft at an average Froude number of 0.23 are presented in Figs. 27(a) and 27(b) respectively. As the vessel moves in water, the bow will experience high pressure at the top and low pressure at the bottom keel portion; in the case of the stern, it experiences suction pressure at the top and low pressure at the bottom keel portion due to eddy currents resulting in a whirling effect due to sudden change in cross-section.

The variation in the wave-making resistance (C_w), friction (C_f) and total resistance (C_T) coefficients and the variation of drag force with the speed of the vessel have been presented in Figs. 28 and 29 respectively. The coefficients of wave-making resistance, frictional resistance, and total resistance exhibit a slight reduction with an increase in speed. This could be because the vessel experiences a lift with an increase in speed, reducing the area of contact with water. The maximum values of the wave, frictional and total drag force are 4350.93kN, 11834.28kN, and 16185.20kN respectively.

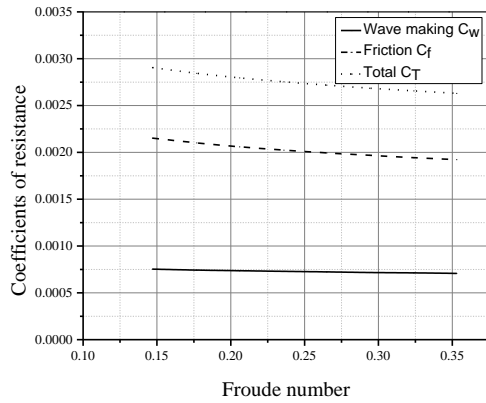


Fig. 28. Plot of coefficients of resistance versus Froude number

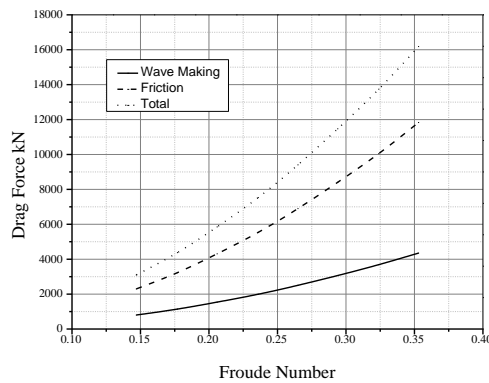


Fig. 29. Plot of drag force versus Froude number

D. Characterisation and CFD Analysis of a Typical House Boat

Hydrodynamic analysis of the houseboat has been performed using the commercial CFD software package SHIPFLOW 6.1®. It employs a cell-centered finite volume-based method (an advanced version of SHIPFLOW from the version SHIPFLOW 5.1® that has been used for Snake boat and Uru). The governing equations like Reynolds averaged Navier Stokes equations are solved numerically using SHIPFLOW by adopting a cell-centered finite volume method. The analysis has been performed by employing coarse, medium and fine meshes for selected drafts of 0.45, 0.475m, 0.5m and 0.525m. The range of Froude numbers was so selected that it corresponds to the entire range of speeds attained by the houseboat. Table 10 and Table 11 has been presented the prototype dimensions and the hydrostatic data pertaining to the houseboat respectively. The total self-weight of the houseboat is 18.416 tonnes taking the thickness of the vessel as 0.2m and surface area 115.124m² relates to a draft of 0.429m.

The XCHAP iteration history plot for 0.5m draft and Froude number of 0.385 has been shown in Fig. 30. The summary of the XCHAP result has been shown in Table 12.

Table 10. Prototype dimensions of the houseboat

Parameter	Length between perpendiculars L_{pp} (m)	Breadth $h(B)$ (m)	Draft (T) (m)	Block Coefficient $t(C_B)$	Surface area (S) (m ²)
Vaues	22.0	4.44	1.3	0.56	6.50

Table 11. Hydrostatic data of House boat

Draft	0.100	0.200	0.300	0.400	0.500	0.600	0.700
Amidships							
m							
Displacement, t	2.401	6.155	10.93	16.56	22.92	29.86	37.33
Draft at FP, m	0.100	0.200	0.300	0.400	0.500	0.600	0.700
Draft at AP, m	0.100	0.200	0.300	0.400	0.500	0.600	0.700
Draft at LCF, m	0.100	0.200	0.300	0.400	0.500	0.600	0.700
WL Length, m							
	21.46	21.89	22.27	22.62	22.95	23.25	23.54
Beam max extents on WL, m	9	0	3	5	2	7	3
Beam max	1.670	2.154	2.522	2.825	3.117	3.380	3.595
Wetted Area, m²							
	31.46	43.31	53.41	62.35	69.95	77.27	83.96
Waterpl. Area, m ²	5	0	6	0	0	6	8
Waterpl. Area, m ²	30.88	41.95	51.00	58.65	64.81	70.46	75.21

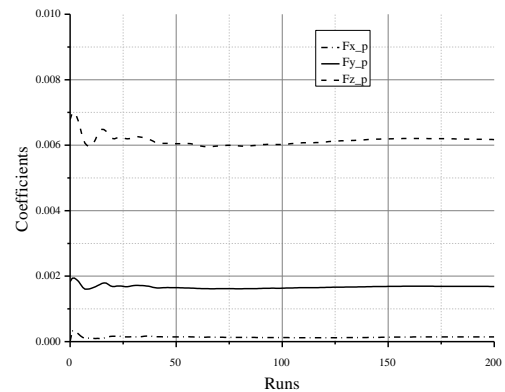


Fig. 30. XCHAP run history plot

Table 12. XCHAP results

Resistance Coefficients	CONDITIONS
C_F (Frictional resist. coeff.)	0.003204 Vm_s (Speed [m/s]) 1.627
C_p (Pressure resist. coeff.)	0.004318 Lref (Reference length [m]) 2.340
C_T (Total resist. coeff.)	0.007522 F_n (Froude number) 0.3396
S (Wetted surface [m ²])	0.1331 R_n (Reynolds number) 32,01,000
HULL DATA	
L_{PP} (Model Lpp [m])	2.340 ρ (Fluid density [kg/m ³]) 1026
S (Wetted area [m ²])	0.7289 η (Fluid viscosity [m ² /s]) 1.189*10 ⁻⁶
	g (Gravity [m/s ²]) 9.807
RESISTANCE	
R_F (Frictional resistance [N])	3.171 R_T (Total resistance [N]) 7.445

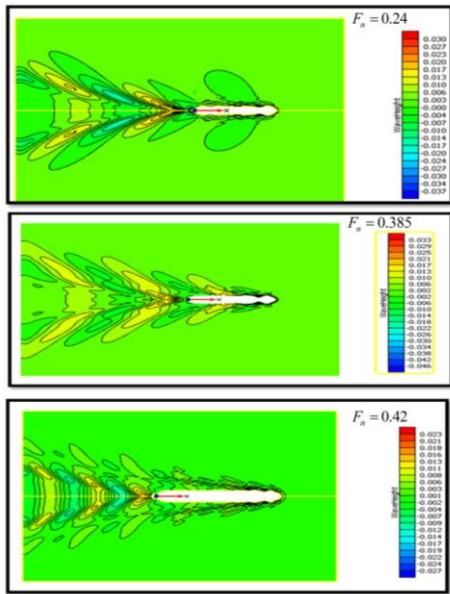


Fig. 31. Kelvin wave pattern at 0.50m draft

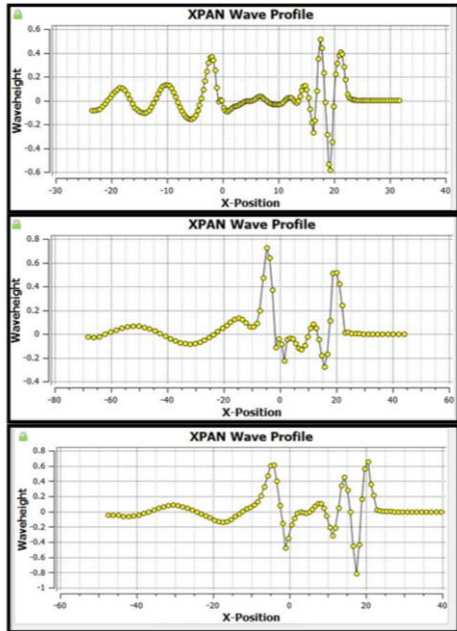


Fig. 32. Wave profiles at 0.50m draft

Fig. 32 shows the wave profiles at Froude numbers 0.24, 0.385 and 0.420 corresponding to a draft of 0.5m. At $F_n = 0.245$, the maximum wave elevation is 0.52m whereas at $F_n = 0.385$, the corresponding value is 0.69m. At $F_n = 0.420$, the maximum wave elevation is 0.75m. From the simulations, it has been observed that generated wave height increases with an increase in the speed of the houseboat. The potential energy carried by water particles increases with wave height and kinetic energy of water particles depends upon the speed of the vessel. As the speed of the boat increases, the potential energy, as well as the kinetic energy possessed by the water particles, increases increasing resistance. The wave profile along the length of the boat has a varying pattern from bow to stern for different Froude numbers on account of varying degrees of turbulence.

The maximum height of the generated wave when the vessel is moving in calm water at different speeds has been observed, the corresponding wave elevation and the elevation of the top of a vessel has been plotted at various Froude

numbers and different drafts (Figs. 33 to Fig. 36). From Fig. 33, it has been observed that the wave is not crossing the top of the vessel, i.e., the vessel generated waves are below the top of the vessel at drafts 0.45m and 0.475m at these Froude numbers. As evident from Fig. 36, for a draft of 0.525m, the ship-generated waves are crossing the top of the vessel beyond a Froude number of 0.56. This means that the vessel is underwater which is unacceptable. Hence the design draft for the vessel has to be limited to 0.5m and this condition shall be strictly adhered to for Froude numbers in the range of 0.21 to 0.56.

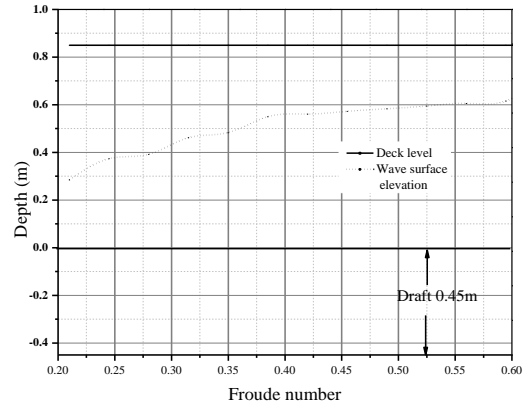


Fig. 33. Froude number versus freeboard for draft = 0.45m

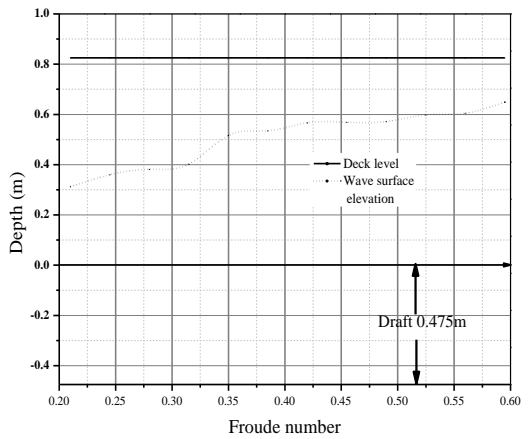


Fig. 34. Froude number versus freeboard for draft = 0.475m

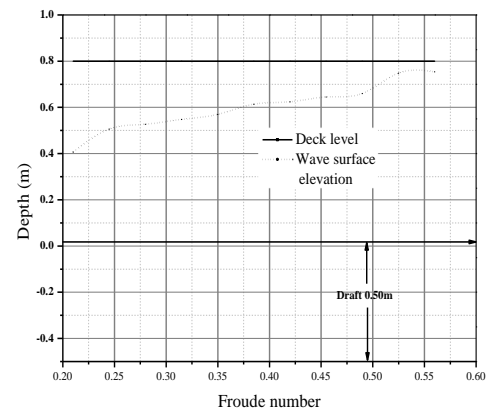


Fig. 35. Froude number versus freeboard for draft = 0.5m

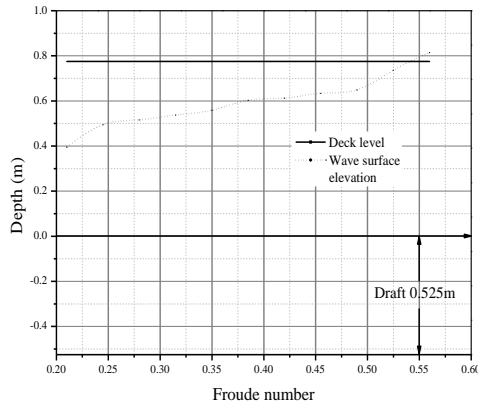


Fig. 36. Froude number versus freeboard for draft = 0.525m

Figs. 37, 38 and 39 present the wave-making resistance, frictional resistance and the total resistance of the houseboat at drafts 0.45m, 0.475m and 0.5m respectively for different Froude numbers. The wave-making resistance increases with an increase in the speed of the boat with some troughs and crests; The frictional resistance also increases with the speed of the boat. At a draft of 0.45m, it has been observed that the maximum wave-making resistance is 8205.73kN, the maximum frictional resistance is 2819.408kN and the total drag is 11025.146kN. At a draft T = 0.5m, the maximum wave-making resistance is 10498.346kN, the maximum frictional resistance is 3262.718kN and the total drag is 13761.146kN. As the draft of the houseboat increases, the surface area of the boat increases by increasing frictional resistance and wave-making resistance.

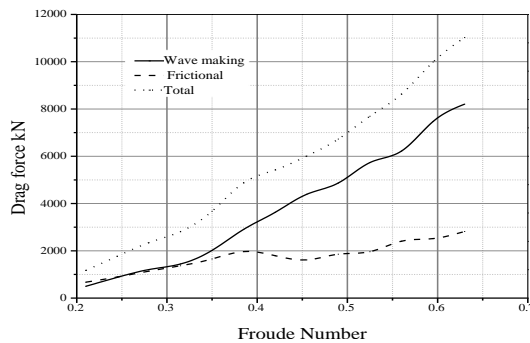


Fig. 37. Froude number versus drag force at draft 0.45m

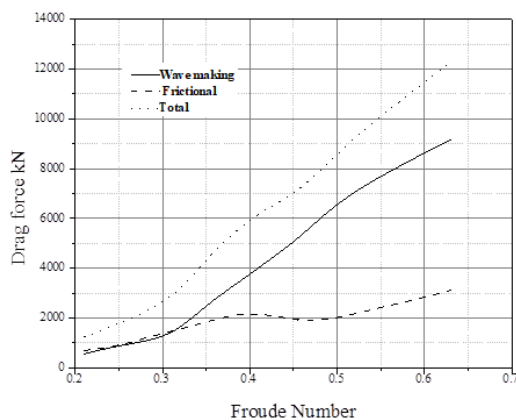


Fig. 38. Froude number versus drag force at draft 0.475m

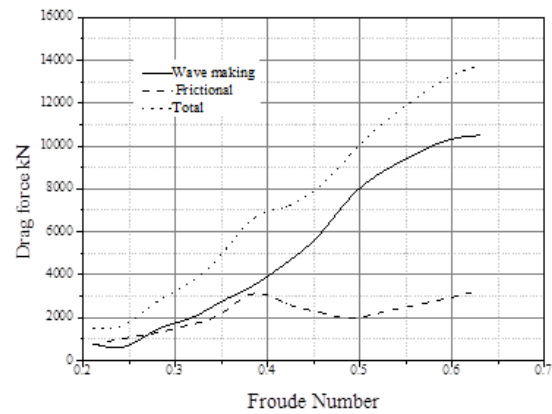


Fig. 39. Froude number versus Drag force at draft 0.50m

Figs. 40 and 41 have been presented the plots of pressure and velocity coefficient contours along the length of the boat

at Froude numbers 0.210, 0.245, 0.385, 0.420, 0.490, 0.525 and 0.560. The non-dimensionalized pressure is extracted through the expression, $p = 0.5C_p p_0$ (measured in Pascal, $p_0 =$ Atmospheric pressure 101325Pa) and the non-dimensionalized velocity is extracted by multiplying velocity coefficients with the ship speed. A C_p value of zero indicates that the pressure is the same as the free stream pressure, a C_p value of one indicates the pressure is stagnation pressure and the point is a stagnation point. The forward stagnation point where the velocity is zero experiences maximum pressure.

Fig. 40(a) shows the pressure on the hull surface $F_n = 0.21$. It can be observed that the starting portion of the bow experiences turbulent suction pressure (15.553MPa) and the ending point of stern experiences positive pressure (16.72MPa). The remaining portion experiences lesser pressure due to uniform surface between A.P. and F.P. From Figs. 40(a) to (g), as the speed increases, the pressure also increases on the surface and bow experiences suction pressure due to passage of water away from the surface. The remaining portions experience the lesser magnitude of pressure due to their uniform shape of the surface. From the velocity profile in Fig. 41(a) at $F_n = 0.21$, it can be seen that there is uniform flow velocity across the entire surface. At bow and stern, dispersion of velocity contours away from the surface is observed. As speed increases, high-velocity profiles can be observed at bow and stern and smaller velocities at other locations. The curvature of the ship is not constant throughout its length and hence the flow velocity changes. At the location of the bow, velocity is zero, technically known as stagnation point. At this point, pressure attains a maximum value and the wave system starts with a crest. Figs. 41(a) to (g) presents the plots of velocity coefficient contours along the length of the boat for Froude numbers ranging from 0.210 to 0.560. It has been observed that velocity remains constant when the curvature of the houseboat is constant. Initially, the velocity at the bow is zero which increases over the surface of the houseboat up to its shoulder region owing to the increase in curvature of the houseboat.

Velocity remains constant beyond shoulder up to aft shoulder location reflective of the constant curvature between these points.

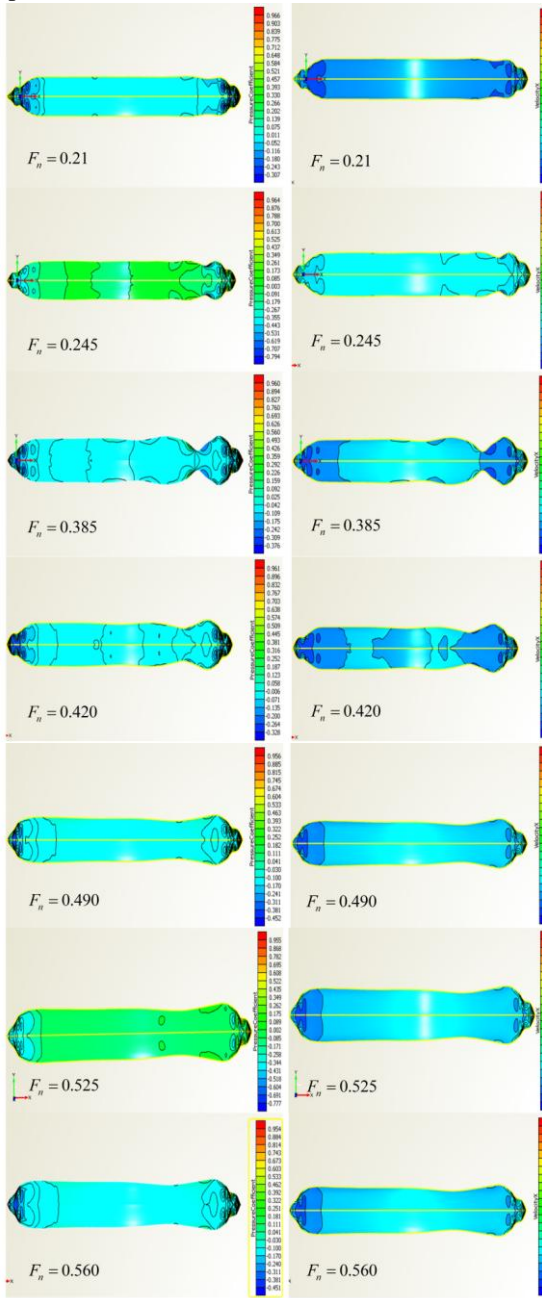


Fig. 40. Pressure coefficient contours

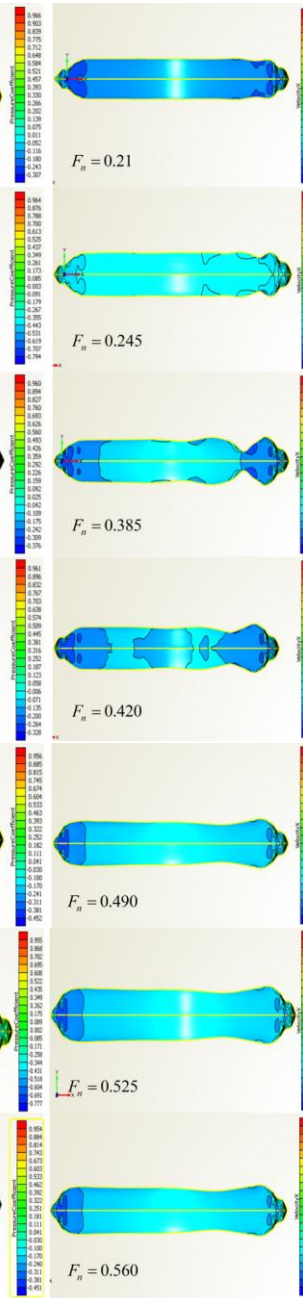


Fig. 41. Velocity coefficient contours

E. Consolidated Results and Comparison with Standard Vessels

One of the primary goals set for this work was the characterization of three traditional vessels of Kerala of which no formal data was available. The coordinate data of these vessels obtained through the Total Station survey has been well documented for future use.

Following the convergence study on the vessel carried out using coarse and medium meshes, the final analysis was carried out using a fine mesh. It has been observed that total resistance increases with an increase in speed and draft of the vessel. Table 13 presents consolidated results of the analysis comparing Snake boat, Uru and houseboat with each other. For Uru,

the ideal draft was found to be 2.4m with the ideal speed range of 6.3kmph to 22.01kmph. For the Snake boat, the ideal draft was found to be 0.5m with the ideal speed range of 12.02kmph to 17.03kmph. For the houseboat, the ideal draft was found to be 0.5m with the ideal speed range of 11.12kmph to 29.63kmph.

Based on the findings, the following suggestions can be given to designers and shipbuilders:

- The ideal draft of the vessels should be maintained for optimal performance
- Care should be taken while loading the vessel so that the draft is maintained
- A physical mark should be placed corresponding to the ideal draft such that it is never violated
- With the ideal draft, the optimal range of speed should be maintained for fuel-efficiency. In the case of the Snake boat, which is used for racing propelled manually, fuel efficiency is indicative of the effort required to be put-in by the rowers in propelling the boat.

From Table 13, it can be inferred that out of the total drag force experienced by a Snake boat at the ideal draft, 66.8% is attributed to the frictional drag and only 33.2% is wave-making resistance drag. These values change to 73.1% and 26.9% respectively for Uru and 23.7% and 76.3% for a houseboat. It means the wave-making resistance drag contributes to about 3/4th of the resistance of a houseboat unlike the case of Snake boat and Uru where the frictional drag plays the predominant role.

With regards to the magnitude of values, the total resistance experience by an Uru when compared to Snake boat and houseboat are 30.16 and 1.17 times respectively. However, these values do not aid in a meaningful comparison of the vessels as the magnitude of the values is a function of the size of the vessel; more the size greater will be the resistance value. A better comparison is obtained using the non-dimensional coefficient of these numbers (C_W , C_F and C_T). The comparative plots of these coefficients are presented in Fig. 42, 43 and 44 for values of Snake boat, Uru and houseboat in addition to the values of some standard vessels obtained from the literature.

Table 13. Consolidated Results

	L_{PP} (m)	B (m)	D (m)	Ideal draft (m)	Range of F_n		Wave drag (kN)	Friction al drag (kN)	Total drag (kN)
					From	To			
Snake Boat	19.69	2.32	0.79	0.50	0.24	0.34	178.20	358.3	536.5
					3.34m/sec	4.73m/sec			
Uru Boat	31.12	10.1	3.92	2.40	0.1	0.35	4350.93	11834.2	16185.2
		4			1.75m/sec	6.11m/sec	8	1	

					22.01kmp				
					6.3kmp/h				
						h			
						11.88knot			
					3.4knots				
						s			
					0.21	0.56			
					3.09m/Se	8.23m/sec			
Hous					c				
eboa	22	4.44	1.30	0.50	11.12kmp	29.63kmp	10498.4	13761.1	
t					h	h	1	3	
						15.99knot			
						6.00knots			
						s			

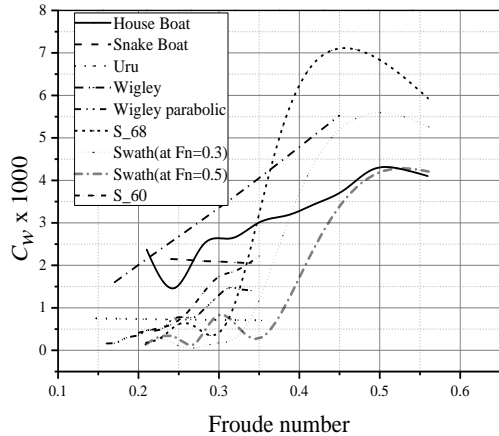


Fig. 42. Cw values versus Froude number compared with standard vessels

From Fig. 42, it is seen that the values of Cw for Snake boat and Uru are in the median range and monotonically decrease slightly with an increase in Froude number unlike most of the standard vessels. For Snake boat and Uru, as the Froude number range was limited to a low value, the variation of Cw for the regime where most of the vessels showed a sudden jump could not be observed. Among the vessels, the houseboat displayed most variations with regards to its trend (increase or decrease). Cw for houseboat at Froude number of 0.21 is the largest when compared to other vessels that dwindle to a minimum amongst the vessels for a Froude number of 0.56 (slightly stooping below Swath).

From Fig. 43, it is seen that the values of CF for Snake boat, Uru and houseboat are in the median range Similar to the trend shown by the former two in Cw, CF values are also monotonically decreasing with an increase in Froude number. Houseboat exhibited variations in trends and despite starting with a median value for a Froude number of 0.21, it decreases to a low value for Froude number of 0.56. A similar trend has been observed in comparison to CT values. The maximum value of CT for houseboat is 0.006 obtained for a Froude number of 0.38.

The Trim angle variation of the three vessels with respect to the Froude number is compared in Fig. 45. As a positive value of the Trim angle indicates its trimming by the bow, Uru has an increasing value of Trim angle up to Froude number of around 0.25 (allowable speed range as mentioned in wave-cut analysis) beyond which it decreases and even attains a negative value closer to -0.65.

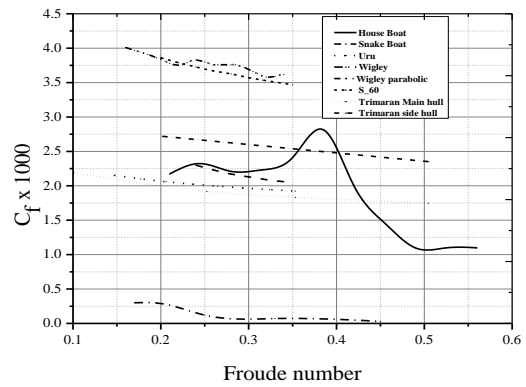


Fig. 43. CF values versus Froude number for Uru compared with standard vessels

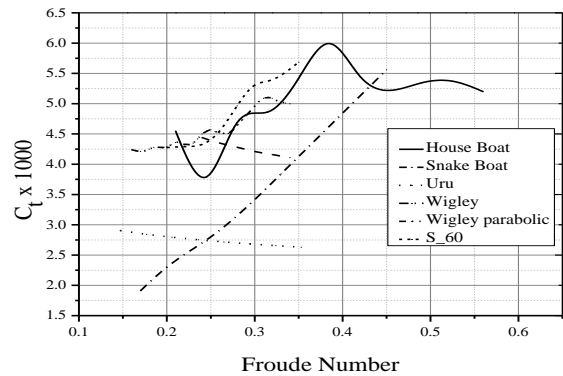


Fig. 44. CT values versus Froude number for Uru compared with standard vessels

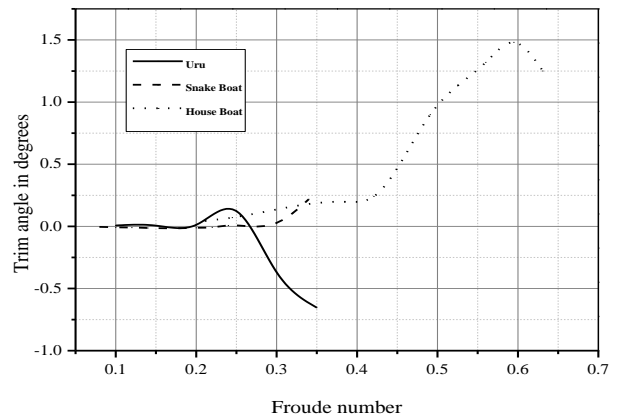


Fig. 45. Trim angle versus Froude number for Uru, Snake boat and houseboat

On comparison, for the Snake boat, the Trim angle increases gradually up to the Froude number of around 0.25. Thereafter, the rate of increase in the Trim angle shoots up. The trim angle variation of the houseboat is similar to Snake boat as it increases in positive value and increases greatly beyond a Froude number of 0.42 before showing a decreasing trend beyond the Froude number of 0.58.

IV. CONCLUSION

In this study, the characterization of three traditional vessels of Kerala, viz., snake boat, Uru and houseboat have been studied.

For Uru, the ideal draft was found to be 2.4m with the ideal speed range of 6.3kmph to 22.01kmph.

For the Snake boat, the design draft for the boat needs to be limited to 0.5m and this condition shall have strictly adhered for Froude numbers from 0.24 to 0.34; wherein, the higher value corresponds to the maximum value of velocity attained 17.03kmph, which marginally falls short of velocity attained by the record holder (19.76kmph) in the long history of snake boat race. For the houseboat, the ideal draft was found to be 0.5m with the ideal speed range of 11.12kmph to 29.63kmph. Designers can use this ideal draft to determine the weight that the vessel can carry.

It can also be concluded that the coefficients of wave-making resistance, frictional resistance, and total resistance exhibit a slight reduction with an increase in speed. The wave-making resistance drag contributes to about 3/4th of the resistance of a houseboat unlike the case of Snake boat and Uru where the frictional drag plays the predominant role. With regards to the magnitude of values, the total resistance experience by an Uru when compared to Snake boat and houseboat are 30.16 and 1.17 times respectively.

It has been found that the presence of the skeg improves the hydrodynamic performance of the houseboat considerably. The absence of skeg has created greater turbulence for the Uru.

The basic requirements of vessels are high stability and low resistance. These requirements can be achieved by subjecting the hull forms to CFD analysis and modifying them based on the results of simulations until the designed performance standards are met. In the Indian scenario, there is ample scope to improve the certification mechanism for vessels, in general, and certain categories of vessels in particular. The study proposed in this work could help in suggesting improvements to the criteria for the certification of vessels, thereby ensuring higher levels of safety.

REFERENCES

- 1 Z. rong ZHANG, H. LIU, S. ping ZHU, and F. ZHAO, "Application of CFD in ship engineering design practice and ship hydrodynamics," J. Hydrodyn., vol. 18, no. 3 SUPPL., pp. 315–322, 2006.
- 2 D. A. Jones and D. B. Clarke, "Fluent Code Simulation of Flow around a Naval Hull: DTMB 5415," p. 34, 2010.
- 3 Ruosi Zha, Haixuan Ye, Zhirong Shen and Decheng Wan "Application of CFD in ship engineering design practice and ship hydrodynamics," J. Hydrodynamics., vol. 18, no. 3, pp. 315–322, 2005.
- 4 Peterson "IIHR-261 Technical Paper" 2003.
- 5 I. ROBERTSON, S. J. SHERWIN, AND J. M. R. GRAHAM, "COMPARISON OF WALL BOUNDARY CONDITIONS FOR NUMERICAL VISCOUS FREE SURFACE FLOW SIMULATION," JOURNAL OF FLUIDS AND STRUCTURES, VOL. 19, NO. 4, PP. 542525, 2004.
- 6 I. Senocak and G. Iaccarino, "Progress towards RANS simulation of free-surface flow around modern ships", Centre for Turbulence Research Annual Research Briefs, pp. 151–156, 2005.
- 7 S. Tarafder, "Third order contribution to the wave-making resistance of a ship at finite depth of water," Ocean Eng., vol. 34, no. 1, pp. 32–44, 2007.
- 8 H. Peng, S. Ni, and W. Qiu, "Wave pattern and resistance prediction for ships of full form," Ocean Eng., vol. 87, pp. 162–173, 2014.
- 9 G. K. Saha, M. A. Miazee, "Numerical and Experimental Study of Resistance, Shrinkage and Trim of a Container Ship," *Procedia Eng.*, vol. 194, pp. 67–73, 2017.
- 10 S. R. CHOUDHURY, A. K. DASH, V. NAGARAJAN, AND O. P. SHAH, "CFD SIMULATIONS OF STEADY DRIFT AND YAW MOTIONS IN DEEP AND SHALLOW WATER," OCEAN ENG., VOL. 142, PP. 161–184, 2017.
- 11 S. LIU AND A. PAPANIKOLAOU, "FAST APPROACH TO THE ESTIMATION OF THE ADDED RESISTANCE OF SHIPS IN HEAD WAVES," OCEAN ENG., VOL. 112, PP. 211–225, 2016.

- 12 X. HUI YANG, H. KUI YE, D. KUI FENG, AND J. LIU, "COMPUTATIONAL RESEARCH ON WAVE MAKING OF MOVING WIGLEY HULL IN TIME DOMAIN," J. HYDRODYNAMICS., VOL. 20, NO. 4, PP. 469–476, 2008.
- 13 S. LUO, N. MA, AND Y. HIRAKAWA, "EVALUATION OF RESISTANCE INCREASE AND SPEED LOSS OF A SHIP IN WIND AND WAVES," J. OCEAN ENG. SCI., VOL. 1, NO. 3, PP. 212–218, 2016.
- 14 Y. K. DEMIREL, O. TURAN, AND A. INCECIK, "PREDICTING THE EFFECT OF BIOFOULING ON SHIP RESISTANCE USING CFD," APPLIED OCEAN RESEARCH., VOL. 62, PP. 100–118, 2017.
- 15 J. E. CHOI, K. S. MIN, J. H. KIM, S. B. LEE, AND H. W. SEO, "RESISTANCE AND PROPULSION CHARACTERISTICS OF VARIOUS COMMERCIAL SHIPS BASED ON CFD RESULTS," OCEAN ENG., VOL. 37, NO. 7, PP. 549–566, 2010.
- 16 K. C. SEO, M. ATLAR, AND D. WANG, "HYDRODYNAMIC DEVELOPMENT OF INCLINED KEEL HULL-PROPULSION," OCEAN ENG., VOL. 63, PP. 90–95, 2013.
- 17 S. TARAFDER AND G. KHALIL, "NUMERICAL ANALYSIS OF FREE SURFACE FLOW AROUND A SHIP IN DEEP WATER," INDIAN JOURNAL OF ENGINEERING & MATERIALS SCIENCES, VOL. 11, NO. OCTOBER, PP. 385–390, 2004.
- 18 F. ZHAO, S. P. ZHU, AND Z. R. ZHANG, "NUMERICAL EXPERIMENTS OF A BENCHMARK HULL BASED ON A TURBULENT FREE-SURFACE FLOW MODEL," COMPUTER MODEL. ENGINEERING SCIENCE, VOL. 9, NO. 3, PP. 273–285, 2005.
- 19 SENOCAK AND G. IACCARINO, "PROGRESS TOWARDS RANS SIMULATION OF FREE-SURFACE FLOW AROUND MODERN SHIPS," CENTER FOR TURBULENCE RESEARCH ANNUAL RESEARCH BRIEFS PP. 151–156, 2005.
- 20 Z. RONG ZHANG, H. LIU, S. PING ZHU, AND F. ZHAO, "APPLICATION OF CFD IN SHIP ENGINEERING DESIGN PRACTICE AND SHIP HYDRODYNAMICS," J. HYDRODYNAMICS, VOL. 18, NO. 3 SUPPL., PP. 315–322, 2006.
- 21 S. AKTAR, G. K. SAHA, AND M. A. ALIM, "DRAG ANALYSIS OF DIFFERENT SHIP MODELS USING COMPUTATIONAL FLUID DYNAMICS TOOLS," INTERNATIONAL. CONFERENCE ON MARITIME TECHNOLOGY., DECEMBER, PP. 123–129, 2010.
- 22 G. TZABIRAS AND K. KONTOGIANNIS, "AN INTEGRATED METHOD FOR PREDICTING THE HYDRODYNAMIC RESISTANCE OF LOW-CB SHIPS," CAD COMPUTER AIDED DESIGN., VOL. 42, NO. 11, PP. 985–1000, 2010.
- 23 C. ALGIE, T. GOURLAY, L. LAZAUSSAS AND H. RAVEN, "APPLICATION OF POTENTIAL FLOW METHODS TO FAST DISPLACEMENT SHIPS AT TRANSCRITICAL SPEEDS IN SHALLOW WATER," APPLIED OCEAN RESEARCH, VOL. 71, PP. 11–19, 2018.
- 24 SHI, M. WU, B. YANG, X. WANG, AND Z. WANG, "RESISTANCE CALCULATION AND MOTIONS SIMULATION FOR FREE SURFACE SHIP BASED ON CFD," *PROCEDIA ENG.*, VOL. 31, PP. 68–74, 2012.
- 25 JOCHEN MARZI. " USE OF CFD METHODS FOR HULLFORM OPTIMISATION IN A MODEL BASIN". MARNET- CFD WORKSHOP, HASLAR 20/21-03-2003.
- 26 ALEX ROBBINS, GILES THOMAS. "VESSEL TRANS-CRITICAL WAVE WAKE, DIVERGENT WAVE ANGLE AND DECAY". INTERNATIONAL JOURNAL OF MARITIME ENGINEERING, 151, 25-38.2009.
- 27 M. PERIĆ AND V. BERTRAM, "TRENDS IN INDUSTRY APPLICATIONS OF COMPUTATIONAL FLUID DYNAMICS FOR MARITIME FLOWS," J. SH. PROD. DES., VOL. 27, NO. 4, PP. 194–201, 2011.
- 28 GIANLUCA LACCARINO, ROBERTO VERZICCO. "IMMERSED BOUNDARY TECHNIQUE FOR TURBULENT FLOW SIMULATIONS". APPLIED MECH REV. 56, 331-347. 2003
- 29 L YU, N. MA, X. GU. "ON THE MITIGATION OF SURF-RIDING BY ADJUSTING CENTER OF BUOYANCY IN DESIGN STAGE". INTERNATIONAL JOURNAL OF NAVAL ARCHITECTURE AND OCEAN ENGINEERING, VOL. 9, NO. 3, PP. 292–304. 2017.
- 30 T. TEZDOGAN, Z. SHENGLONG, Y. K. DEMIREL, W. LIU, X. LEPING, L. YUYANG, R. E. KURT, E. B. DJATMIKO, A. INCECIK. "AN INVESTIGATION INTO FISHING BOAT OPTIMIZATION USING A HYBRID ALGORITHM". OCEAN ENGINEERING, VOL. 167, NO. 1, PP. 204–220, 2018.
- 31 TAYLAN, M. "OVERALL STABILITY PERFORMANCE OF ALTERNATIVE HULL FORMS". OCEAN ENGINEERING 29, 1663-1681. 2001.
- 32 TAYLAN, M. "STATIC AND DYNAMIC ASPECTS OF A CAPSIZE PHENOMENON". OCEAN ENGINEERING 30, 331–350. 2002

- 33 Y. SINGH, S K BHATTACHARYYA AND V. G. IDICHANDY, "CFD APPROACH TO MODELLING, HYDRODYNAMIC ANALYSIS AND MOTION CHARACTERISTICS OF A LABORATORY UNDERWATER GLIDER WITH EXPERIMENTAL RESULTS," JOURNAL OF OCEAN ENGINEERING AND SCIENCE, VOL. 2, NO. 2, PP. 90-119, 2017.
- 34 SURENDRAN, S., VENKATA RAMANA REDDY, J. "NUMERICAL SIMULATION OF SHIP STABILITY FOR DYNAMIC ENVIRONMENT", OCEAN ENGINEERING 30, 1305-1317. 2003
- 35 H. B. MORAES, J. M. VASCONCELLOS AND R. G. LATORRE, "WAVE RESISTANCE OF HIGH-SPEED CATAMARANS," OCEAN ENGINEERING, VOL. 31, NO. 17-18, PP. 2253-2282, 2004.
- 36 [HTTPS://EN.WIKIPEDIA.ORG/WIKI/URU_\(BOAT\)](https://en.wikipedia.org/wiki/URU_(boat))
- 37 "SHIPBUILDING IN BAYPORE PORT". [HTTP://WWW.AMARTYA.DE/BEYPORE1.HTM](http://www.amartya.de/beypore1.htm). DEC-2015.
- 38 [HTTP://SHODHGANGA.INFLIBNET.AC.IN/BITSTREAM/10603/36439/8/CHAPTER%203.PDF](http://shodhganga.inflibnet.ac.in/bitstream/10603/36439/8/CHAPTER%203.PDF)
- 39 R. MATHEN, "HOUSEBOATS IN KERALA - CONSTRUCTIONAL FEATURES AND ENVIRONMENTAL ISSUES," J. ENVIRON. SCI. TOXICOL. FOOD TECHNOL., VOL. 1, NO. 6, PP. 31-43, 2012.
- 40 FENG ZHAO., SONG-PING ZHU., ZHI-RONGZHANG. "NUMERICAL EXPERIMENTS OF A BENCHMARK HULL BASED ON A TURBULENT FREE-SURFACE FLOW MODEL". TECH SCIENCE PRESS.CMES 9. 273-285. 2005.
- 41 [HTTPS://EN.WIKIPEDIA.ORG/WIKI/NEHRU_TROPHY_BOAT_RACE](https://en.wikipedia.org/wiki/Neeru_Trophy_Boat_Race).

in Offshore Engineering. He has been part of numerous research and consultancy projects during his career. His areas of interest include Structural Analysis, Computational Methods, Structural Dynamics and Finite Element Methods. He continues to remain active professionally even after his retirement from the services of NITC.



Dr. M Abdul Akbar is currently working as Assistant Professor at National Institute of Technology Jalandhar. He has over 5 years of industrial experience and 3 years of teaching experience. He obtained his B-Tech in Civil Engineering from National Institute of Technology Calicut, M-Tech in Structural Engineering from Indian Institute of Technology Bombay and Ph.D. in Wind Energy from National Institute of Technology Calicut. His research interests are: Finite Element Analysis, Composite materials, Fatigue Analysis, Structural Dynamics, Non-linear Analysis, Codal guidelines of IS:1893 and IS:875(3), Blast Resistant Design, Smart Materials, Wind Energy and Vertical Axis Wind Turbines.

AUTHORS PROFILE



Mr. B Venkata Subbaiah is currently working as Head of Civil Engineering Section at Smt. Durgabai Deshmukh Government Women's Technical Training Institute (SDDGWTTI), Hyderabad, in the Department of Technical Education. He has 2 years of industrial experience and 21 years of teaching experience in the Department of Technical Education, Telangana. He obtained his B-Tech in Civil Engineering from Jawaharlal Nehru Technological University (JNTU) Anantapur, Andhra Pradesh, M-Tech in Offshore Structures from National Institute of Technology Calicut, Kerala under QIP (full time sponsored programme), and Joined as Research Scholar at National Institute of Technology Calicut, Kerala under QIP (full time sponsored programme). He has guided many Civil Engineering Projects in Diploma level, His research interests are: Design of Offshore Structures, Structural Dynamics, Computational Fluid Dynamics, Ship Design, Non-linear Analysis.



Dr. Santosh G Thampi is currently working as Professor (HAG) in the Department of Civil Engineering at the National Institute of Technology Calicut. He has published many peer reviewed papers in reputed international journals and is a reviewer for many national and international journals. His research interests are: Fluid Mechanics and Hydraulics, Pipe and Channel Flows, Hydrologic Processes and Modelling, Water Quality Modelling, Water and Wastewater Treatment, Application of Remote Sensing and Geographical Information Systems in Natural Resources Management, Economics of Water Resources Systems, Water Resources Systems Analysis & Management and Coastal Processes and Hydrodynamics. He is a member of several leading professional societies and has successfully completed many externally funded projects.



Mr. Nimma Rambabu is currently working as Assistant Professor at Indira Gandhi Institute of Technology Sarang, Odisha. He has over 2 years of teaching experience. He obtained his B-Tech in Civil Engineering from Bapatla Engineering college Bapatla, M-Tech in Offshore Structures from National Institute of Technology Calicut. His research interests are: Computational Fluid Dynamics, Ship Design, Structural Dynamics, Non-linear analysis, Expansive Soils, Soil dynamics and Design of Offshore Structures.



Dr. V Mustafa retired as Professor in Civil Engineering from the National Institute of Technology Calicut. He was also Dean (Planning and Development) for a term at NITC. He completed his B.Sc. (first rank) in Civil Engineering from University of Calicut and M-Tech (gold medalist) in Structural Engineering from Indian Institute of Technology Madras and Ph.D. from Indian Institute of Technology Madras